Segregation-considered feature analysis of the Zn diffusion in InGaAs/InAlAs/InP heterostructures

© P.E. Kopytov[1], I.A. Starkov[2], I.I. Novikov[1], S.A. Blokhin[3], D.S. Papylev[1], R.V. Levin[3], V.V. Andryushkin[1], Ya.N. Kovach[3], E.V. Nikitina[4], K.O. Voropaev[5], A.F. Tsatsulnikov[6], L.Ya. Karachinsky[1]

[1] ITMO University,
St. Petersburg, Russia
[2] R&D Center of Thin Film Technologies in Energetics under the Ioffe Institute LLC,
St. Petersburg, Russia
[3] Ioffe Institute,
St. Petersburg, Russia
[4] Alferov Federal State Budgetary Institution of Higher Education
and Science Saint Petersburg National Research Academic University of the Russian Academy of Sciences,
St. Petersburg, Russia
[5] OAO OKB-Planeta,
Veliky Novgorod, Russia
[6] Submicron Heterostructures for Microelectronics Research and Engineering Center
of the Russian Academy of Sciences,
St. Petersburg, Russia

E-mail: kopytovpe@itmo.ru

Received February 4, 2026
Revised March 2, 2026.
Accepted March 20, 2026

This paper presents segregation-considered diffusion model of Zn dopants in InGaAs/InAlAs/InP heterostructures, which makes it possible to calculate the qualitative and quantitative evolution of the Zn concentration profile. A wide range of experimental data has been analyzed for various technological regimes of Zn diffusion into InGaAs/InAlAs/InP heterostructures in a metalorganic chemical vapor deposition reactor using diethylzinc as the diffusant source. The influence of temperature and pressure on the diffusion and segregation coefficients is determined. It is demonstrated that ignoring segregation processes in diffusion model can lead to a significant error in determining the diffusion coefficients. The Zn diffusion profiles are calculated depending on the thickness of InGaAs/InAlAs/InP heterostructure layers and technological regimes of diffusion process. It has been demonstrated that the use of solid solution layers, even those of relatively small thickness, can significantly change the depth of diffusion penetration due to the low diffusion coefficient and the large gradient of the segregation coefficient.

Keywords: diffusion, segregation, dopant, diethylzinc, indium phosphide.

DOI: 10.61011/SC.2026.01.63721.9058

1. Introduction

Diffusion of zinc (Zn) into III-V heterostructures is a widely used process for the fabrication of electronic and optoelectronic devices [1–3]. Technologically, the diffusion process occurs locally through a dielectric mask using one of the following methods: diffusion in a sealed ampoule [4], diffusion of Zn from an applied coating [5], diffusion of Zn through a narrow gap using a planar source [6], or diffusion from the vapor phase in an open tube [7]. The latter method has proved to be efficient due to high homogeneity of the diffusion process over the sample area while maintaining the reproducibility of the results obtained.

The main parameters that influence Zn diffusion profile are diffusion conditions, the type of diffusant, the process method and the type of reactor used [7]. Unfortunately, in the literature there are only a few theoretical and experimental works that comprehensively examine the dependence of the diffusion depth on the listed parameters. It is obvious that mathematical modeling of diffusion processes in real heterostructures enhances and accelerates the research process. In addition, the mathematical model also enables to identify features and details of processes that are difficult to detect in a real experiment.

Studies of Zn diffusion process in heterostructures based on III-V compounds rely on complex approaches to the analysis of dopant distribution profiles and interface characteristics. Scanning electron microscopy (SEM) is the most direct method for assessing Zn diffusion depth by identifying the image contrast boundary between regions of the semiconductor with different types of charge carriers [8–10]. However, the distribution of electric field across the cross-section of the sample affects the contrast of SEM image and the accuracy of determining the depth of Zn dopant occurrence. Thus, this method is optimal for monitoring the formation of a double doping front [7,11]. Secondary-ion mass spectrometry (SIMS) provides information on the distribution profile of Zn atoms embedded in InP [7,12–14]. Such information is widely used to model the diffusion process [15]. However, in practice, it is often necessary to

know the actual distribution of electrically active dopants in the heterostructure, the concentration of which can greatly depend on the type of Zn diffusion process and its parameters in combination with the design of heterostructure itself. The solution to this problem involves the use of a less resource-intensive method of electrochemical capacitance-voltage profiling (ECV) [16]. Although the amount of electrically active dopants may differ significantly from the concentration of embedded atoms during Zn vapor phase diffusion [12,17], the use of *in situ* or *ex situ* thermal activation of dopants allows one to obtain a good correlation of the distribution profile of electrically active dopants obtained by ECV method with the distribution profile of embedded Zn atoms obtained by SIMS method [14,18].

For a long time, the influence of segregation processes on Zn diffusion profile was ignored in the scientific literature and was often explained by measurement errors or physical artifacts [12,17,19]. An earlier ECV study of Zn diffusion into InP through the InGaAs surface layer revealed segregation of the dopants near InGaAs–InP [11] heterointerface. In [20] that gives an insight on Zn diffusion into InGaAs/InP/InAlAs/InP heterostructure, a combination of time-of-flight SIMS, magnetic SIMS and high-energy X-ray photoelectron spectroscopy methods was used to discover effective blocking of Zn diffusion into InP by means of InAlAs layer.

Previously, using the results of ECV analysis of InGaAs/InP heterostructures subjected to Zn vapor phase diffusion, an approach was developed for modeling the process of Zn diffusion into InGaAs/InP heterostructures accounting for the dopant segregation [21]. Based on the previously developed approach, in this study a comprehensive theoretical analysis of experimental data on Zn diffusion from the vapor phase in InGaAs/InAlAs/InP heterostructures was carried out in order to determine the effect of a thin (~ 10 nm) InAlAs etch-stop layer exerted on the dopant occurrence depth.

2. Diffusion-segregation model of Zn distribution

In solid-state structures, the diffusion of dopants or point defects of various natures occurs simultaneously with the segregation process. As a result, for precise modeling of the concentration distribution of N_a dopant, it is necessary to consider both of these phenomena [22–24]. Similar to classical Fick's laws, the general diffusion-segregation equation can be obtained on the basis of thermodynamic principles and has the following form [24,25]:

$$\frac{\partial N_a(x,t)}{\partial t} = \frac{\partial}{\partial x}\left[D(x,t)\left(\frac{\partial N_a(x,t)}{\partial x} - \frac{N_a(x,t)}{m(x)}\frac{\partial m(x)}{\partial x}\right)\right], \quad (1)$$

where x — depth, t — time, D — effective diffusion coefficient, m — dimensionless segregation coefficient. Due to the presence of interstitial and vacancy mechanisms of Zn diffusion into InP, InGaAs/InP and InGaAs/InAlAs structures, the effective diffusion coefficient D turns out to be dependent on the dopant concentration $N_a(x,t)$ [12,26]:

$$D(x,t) = D_0\left(\frac{N_a(x,t)}{N_0}\right)^n. \quad (2)$$

The parameters D_0 and N_0 determine the diffusion coefficient and dopant concentration on the surface of heterostructure (analogue of the source). The mathematical notation of equation (1) enables to normalize the segregation coefficient $m(x)$ to the value on the surface of heterostructure $m(0)$ without making any additional changes. This transformation significantly simplifies the process of finding diffusion-segregation parameters from experimental data.

To fully formulate the diffusion-segregation problem, it is necessary to formulate the boundary conditions. The corresponding boundary and initial conditions are as follows:

$$N_a(x,0) = 0, \quad N_a(0,t) = N_0, \quad \frac{\partial N_a(H,t)}{\partial x} = 0, \quad (3)$$

where H is the total thickness of the heterostructure, and the origin of coordinates corresponds to the interface between the vapor phase and heterostructure surface. The numerical solution of equations (1)–(3) was carried out in Comsol Multiphysics using the differential mathematics module.

3. Experimental samples and research methods

To find the evolution of the spatial distribution of $N_a(x,t)$ dopant concentration for a given source N_0, it is necessary to know the parameters of the heterostructure D_0 and $m(x)$. While average values of diffusion coefficients can be found in the scientific literature, the dependence of the segregation coefficient on the depth of dopant occurrence is unique for the growth in every specific process. As a simple solution, this information can be found by reproducing the experimental dependences of the dopant concentraion $N_a(x,t)$ in heterostructures based on InAlGaAs/InP material system, taking into account the features of Zn diffusion method and the final instrumentation application.

When implementing Zn diffusion from the vapor phase, dimethylzinc (DMZn) or diethylzinc (DEZn) is typically used as Zn source. However, in the first case, because of a high background level of diffusant sustained in the reactor for a long time it is required to provide a separate setup solely for this task. Whereas in the second case, the low limiting doping level of InP leads to the problem of forming an ohmic p-contact to InP:Zn layers (typically the doping level does not exceed $2 \cdot 10^{18}$ cm^{-3}). To solve this problem, an additional InGaAs layer is introduced into the heterostructure, the solubility limit of Zn in which is several orders of magnitude higher than in InP [13]. It is worth considering that thickness of InGaAs layer and its lateral size significantly affect the rate and depth of diffusion of Zn into InP through InGaAs [27].

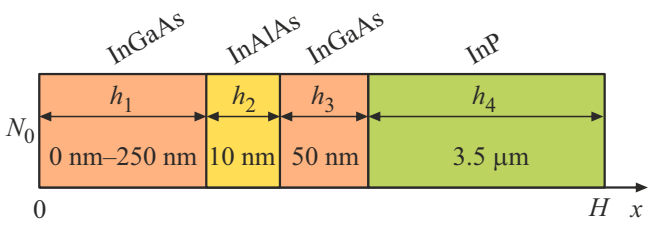

Figure 1. Schematic representation of the studied InGaAs/InAlAs/InP heterostructure.

When creating planar avalanche photodiodes (APD) with separate regions of photon absorption and multiplication of photogenerated charge carriers, including for the detection of single photons, it is necessary to form a double front of p-type dopant [28]. However, the local formation of a double front of p-type dopant in two Zn diffusion processes, necessary for the operation of APD, is associated with problems of modifying the semiconductor surface during the formation of a dielectric mask, leading to an increase in the dark currents of APD [27]. An alternative method for forming a two-stage profile of p-type dopant in a single Zn diffusion process is the formation of a surface relief [7,10]. However, the use of plasma-chemical methods for etching a semiconductor is associated with the risk of damaging the surface and generating crystalline defects in the multiplication layer [29], while non-selective chemical etching does not ensure uniformity and reproducibility of relief etching both in area and in depth. The solution to this problem is associated with the use of selective chemical etching and InAlAs stop layers. The final structure of the experimental samples is a four-layer system consisting of a surface layer of undoped InGaAs $h_1 = 250$ nm thick, a stop layer of undoped InAlAs $h_2 = 10$ nm thick, a layer of undoped InGaAs $h_3 = 50$ nm thick, and a layer of undoped InP $h_4 = 3.5\,\mu$m thick. InGaAs/InAlAs/InP heterostructures of mentioned design were grown on InP substrates using metal-organic chemical vapor deposition (MOCVD). Schematic representation of this design is illustrated in Figure 1. Subsequently, to analyze the influence of h_1 thickness on the diffusion depth, the grown structures were subjected to successive dry etching of InGaAs surface layer (i. e. $h_1 = 200$, 150, 100, 50, 0 nm).

Zn vapor phase diffusion in InGaAs/InAlAs/InP heterostructures occurred in the MOCVD reactor Aixtron AIX-200. DEZn was used as a metal-organic source of Zn. Zn diffusion process was carried out at 475–500 °C and pressure reactor of 50–200 mbar. After Zn diffusion process, the studied heterostructures were subjected to *ex situ* rapid thermal annealing in a nitrogen flow for 5 min at a temperature of 450 °C for thermal activation of dopants.

One-dimensional distribution profiles of electrically active dopants in heterostructures subjected to Zn diffusion process were obtained by ECV method using a Nanometrics ECVpro electrochemical profilometer.

4. Results and discussion

4.1. Determination of diffusion and segregation coefficients

The one-dimensional distribution profiles of electrically active dopants $N_a(x,t)$ in InGaAs/InAlAs/InP heterostructures measured by ECV method under various process conditions are shown in Figure 2. In the diffusion process, the dopant concentration experiences a jump at the interfaces caused by the phenomenon of segregation in heterogeneous layers. To reproduce the obtained dependencies using model (1)–(3), the concentration of the source N_0 was determined from the experimental dependencies $N_a(x,t)$ at $x = 0$. As a result of minimizing the square of the error between the calculated value and the actual value $N_a(x,t)$, the curves of diffusion coefficients D_0 versus temperature and pressure in the reactor were plotted for each heterostructure material (see Figure 3, *a*). Also, the segregation coeffient versus dopant occurrence depth $m(x)$, were also found as illustrated in Figure 3, *b*. In this case, the behavior of $m(x)$ dependences for all the considered thicknesses of InGaAs surface layer is identical, and for each case it can be obtained using proportional scaling of the dependences shown in Figure 3, *b*. Figure 3, *b* shows that pressure, temperature and type of material have a significant effect on $m(x)$. Thus, increasing the temperature from 475 to 500 °C at a fixed reactor pressure of 50 mbar leads to a decrease in the values of the segregation coefficient in all layers of the heterostructure while maintaining a noticeable dip in $m(x)$ dependence at the interface between the surface layer of InGaAs and InAlAs. Hence, with such process parameters, the weakest influence of segregation and a decrease in the depth of occurrence of Zn dopants in InP layer are observed. Increasing the reactor pressure from 50 to 200 mbar while maintaining the temperature 500 °C enhances the segregation coefficient in all layers of the heterostructure, while the previously observed jump at the interface between the surface layer of InGaAs and InAlAs is practically leveled out, which suppresses the blocking of Zn diffusion into the second InGaAs layer and, as a consequence, increases the dopant occurance depth in InP layer.

The table shows the values of diffusion coefficients D_0, reconstructed from ECV measurement data for various process parameters of Zn diffusion. For InP and InGaAs materials, it was found that in the temperature range 475–500 °C and pressures of 50–200 mbar, D_0 rises with both increasing temperature and pressure in the reactor. In case of InAlAs, at the same temperatures and pressures, D_0 rises with increasing reactor pressure, while increasing reactor temperature does not have a significant effect on D_0. The temperature dependence of the diffusion coefficient is consistent with the model described in the literature [30]. At the same time, in the described model, pressure also affects the value of D_0, and an increase in pressure should lead to a lower D_0 due to a declined activation entropy of the diffusion process [31]. However, in this system for InP

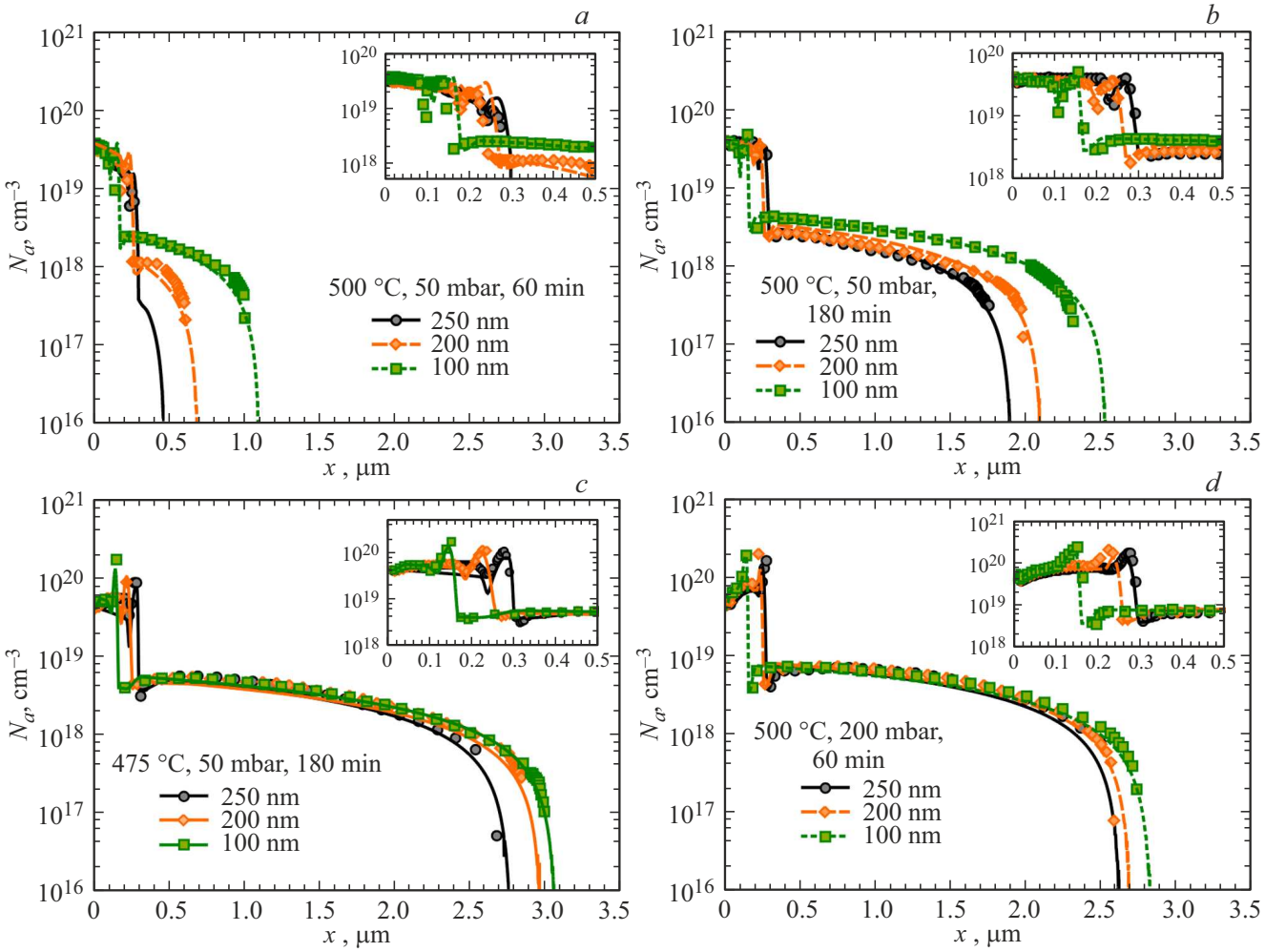

Figure 2. Distribution of profiles of electrically active dopants of *p*-type in InGaAs/InAlAs/InP heterostructure for various thicknesses of InGaAs h_1 surface layer. Symbols — experiment, lines — numerical calculation. *a* — temperature — 500 °C, pressure — 50 mbar, process time — 60 min; *b* — temperature — 500 °C, pressure — 50 mbar, process time — 180 min; *c* — temperature — 475 °C, pressure — 50 mbar, process time — 180 min; *d* — temperature — 500 °C, pressure — 200 mbar, process time — 60 min.

Diffusion coefficients D_0 set within the diffusion-segregation model

Process parameters	InGaAs	InAlAs	InP
$T = 475\,^{\circ}\mathrm{C}$, $P = 50$ mbar	$1.3 \cdot 10^{-13}$ cm^2/s	$4.0 \cdot 10^{-13}$ cm^2/s	$3.0 \cdot 10^{-11}$ cm^2/s
$T = 500\,^{\circ}\mathrm{C}$, $P = 50$ mbar	$1.4 \cdot 10^{-13}$ cm^2/s	$6.3 \cdot 10^{-13}$ cm^2/s	$4.8 \cdot 10^{-11}$ cm^2/s
$T = 500\,^{\circ}\mathrm{C}$, $P = 200$ mbar	$7.7 \cdot 10^{-13}$ cm^2/s	$6.2 \cdot 10^{-13}$ cm^2/s	$6.1 \cdot 10^{-11}$ cm^2/s

and InGaAs materials, the opposite effect is observed, which can presumably be associated with a change in the diffusion mechanism from a vacancy to interstitial one [32].

The values D_0 published in the literature for different methods of Zn diffusion in InP vary within the limits of ± 1 order from the result obtained in this study. Thus, for the diffusion from Zn_3P_2 in the sealed ampule the value D_0 for the non-doped InP amounts to $1.4-1.6 \cdot 10^{-10}$ cm^2/s at 550 °C [33,34], and when the diffusant is replaced by Zn_3As_2 at 500 °C makes $\sim 1.3 \cdot 10^{-12}$ cm^2/s [35]. If the duffusant is taken from Zn-containing coatings (such as Demesol, $ZnCl_2$, $Zn(NO_3)_2$, Zn_2SiO_4) at 550 °C, D_0 amounts to $\sim 1.7-2.7 \cdot 10^{-10}$ cm^2/s [36–38]. For the vapor phase diffusion when using DMZn the value D_0 at 500 °C and a flow of 200 cm^3/min makes $\sim 6-8 \cdot 10^{-11}$ cm^2/s [39]. It is worth noting that in the same paper [39] a decrease in the value of D_0 was found to occur at a temperature elevation from 500 to 570 °C. This behavior can be associated with the following effect: as the temperature rises, the proportion of Zn atoms diffusing into the substrate goes down, while the proportion of Zn atoms evaporating from the substrate rises, which in turn leads

to a simultaneous decrease in the surface concentration of Zn and the diffusion coefficient. A similar phenomenon was observed using DEZn as a source of *p*-type dopant in InP directly during the growth process in MOCVD setup [40].

As noted above, the effect of segregation is weakest at a temperature of 500 °C and a pressure of 50 mbar. In this mode of Zn diffusion from the vapor phase, the features (peaks and troughs) of Zn concentration distribution at the interfaces are least noticeable. Such behavior can be described within a simple diffusion model (1)–(3) without taking into account the contribution of segregation (i. e., at $m(x) = 0$). In this case, the coefficients D_0 that allow the experiment to be reproduced must be determined again: InGaAs — $1.6 \cdot 10^{-13}$ cm^2/s, InAlAs — $3.9 \cdot 10^{-15}$ cm^2/s, InP — $2.3 \cdot 10^{-11}$ cm^2/s. Figure 4 shows a comparison of the experimental and calculated data on the evolution of the concentration profile $N_a(x, t)$ for the above-defined D_0 values for samples with thickness h_1 equal 100 and 250 nm. Despite the adequate match between the simulation results and the experimental data, even in this case the diffusion coefficient in InAlAs layer turns out to be underestimated by almost 2 orders of magnitude compared to the diffusion-segregation model (see table), which actually compensates for the absence of the segregation coefficient $m(x)$ in the simple diffusion model. This fact indicates the need to use a diffusion-segregation model when modeling Zn diffusion in InGaAs/InAlAs/InP heterostructures to eliminate errors in determining diffusion coefficients.

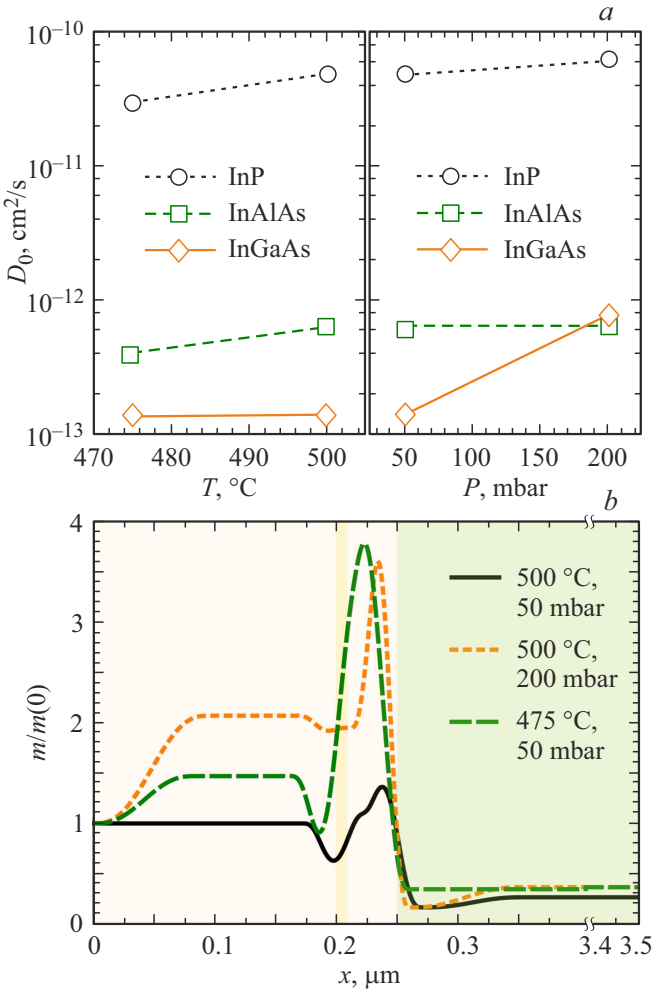

Figure 3. *a* — diffusion coefficient of InGaAs, InAlAs and InP layers versus temperature (pressure is fixed, 50 mbar) and pressure (temperature is fixed, 500 °C); *b* — dimensionless segregation parameter versus dopant occurrence depth at different process parameters in case of InGaAs surface layer thickness of $h_1 = 200$ nm. The color fill corresponds to the boundaries of the heterostructure layers.

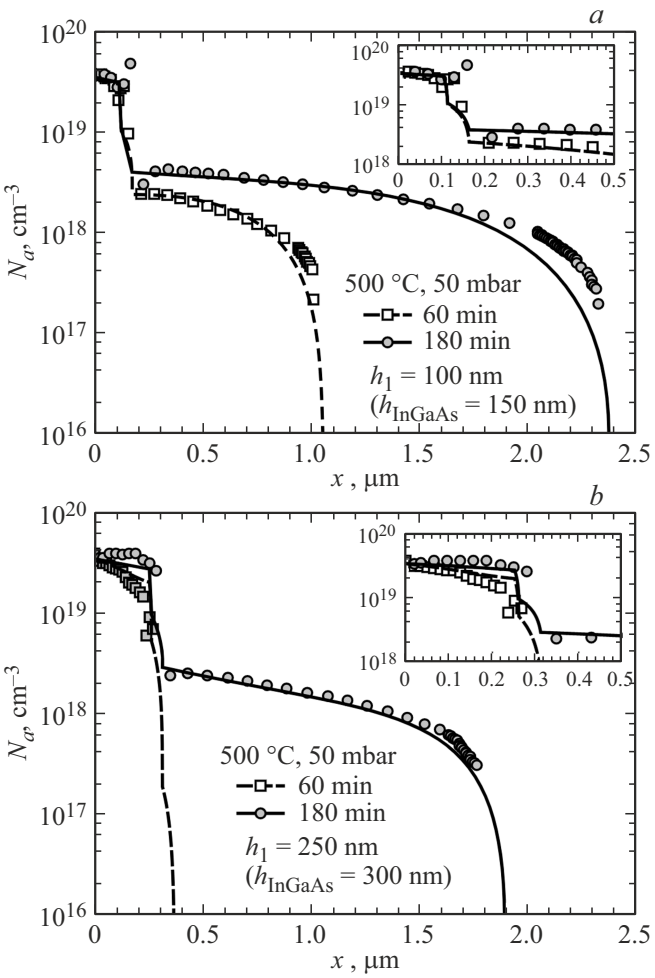

Figure 4. Distribution profiles of electrically active *p*-type dopants in InGaAs/InAlAs/InP heterostructure with an InGaAs surface layer thickness of $h_1 = 100$ nm (*a*) and $h_1 = 250$ nm (*b*). Temperature — 500 °C, pressure — 50 mbar, process time — 60 and 180 min. Symbols — experiment, lines — numerical analysis without segregation, $m(x) = 0$.

4.2. Modelling of Zn diffusion depth

For a given heterostructure design, changing the diffusion coefficients that determine the depth of doping occurrence is possible by selecting the temperature regime and pressure

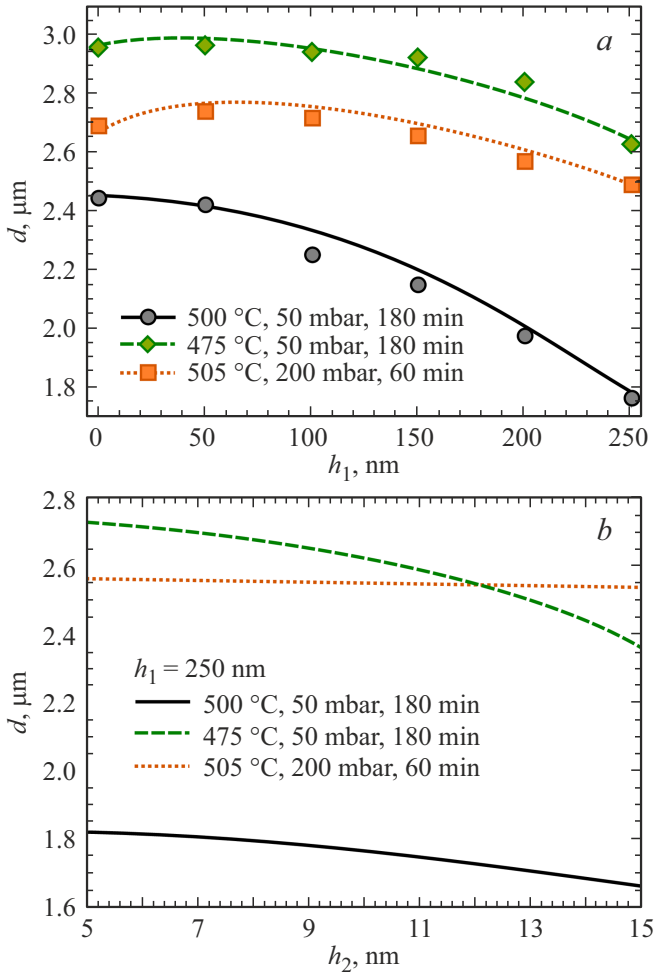

Figure 5. Zn diffusion depth in InGaAs/InAlAs/InP heterostructures versus the surface layer thickness h_1 (a) and thickness of the etch-stop layer h_2 (b) at different process parameters. Symbols — denote the experimental data, lines — denote the data obtained from calculation.

in the reactor. An additional possibility for changing the diffusion depth d is to vary the design of the heterostructure, and in our case, to change the thickness of the solid solution layers. When analyzing the doping profiles with different thicknesses of solid solution layers within this study, the diffusion depth was determined by the position of the front with a concentration equal to $3 \cdot 10^{17}$ cm^{-3}.

In Figure 5, a, experimental and calculated dependences of the depth of Zn dopant occurrence on the thickness of InGaAs surface layer are plotted for all the considered temperatures and pressures in the reactor. Thicknesses of other layers remained unchanged ($h_2 = 10$ nm, $h_3 = 50$ nm, $h_4 = 3.5\,\mu$m). For the process parameters with a temperature of 500 °C and a pressure of 200 mbar, it is worth paying attention to the obvious decrease in the depth of the diffusion front at small h_1. This pattern is characteristic of higher segregation and presence of InAlAs etch-stop layer, which has the lowest diffusion coefficient in these process parameters. From this standpoint, of particular interest is the study of the change in d from the thickness of the etch-stop layer h_2 while fixing the rest of the structure ($h_1 = 250$ nm, $h_3 = 50$ nm, $h_4 = 3.5\,\mu$m). Due to the small thickness of this layer, it is often neglected when conducting various assessments of the diffusion process. According to the modeling results, dependencies $d(h_2)$, presented in Figure 5, b, even with minor changes in the thickness of InAlAs etch-stop layer, can have a noticeable effect on the diffusion depth of Zn in InP under certain process parameters. In the considered case, the greatest relative change in the value of d ($\sim 12\,\%$) with a variation in the thickness of InAlAs etch-stop layer by 5 nm is observed at a temperature of 475 °C and a pressure of 50 mbar. A rise in temperature and/or pressure at which the diffusion process occurs leads to a weakening of the effect of Zn diffusion into InP blocking by InAlAs etch-stop layer because of the increased diffusion coefficients D_0.

In turn, varying the thickness h_3 of the second InGaAs layer does not lead to a noticeable change in d. Thus, a double thickness growth of this layer leads to a change in the diffusion depth of only 2–3 % depending on the process parameters. Such a small effect of thickness h_3 on the diffusion depth can be associated with the presence of Zn segregation at InGaAs/InP interface under all the studied process parameters. When h_3 is varied, the dopant concentration in the layer remains high, which means that the condition for overcoming the interface is preserved, as a result of which no large change in the diffusion depth is observed. For this reason, these results are not presented in this paper. It can be concluded that the performed numerical analysis demonstrates the need to consider a complete heterostructure design (i. e., a four-layer system InGaAs–InAlAs–InGaAs–InP) to adequately reconstruct the evolution of Zn concentration distribution profile from the experiment.

5. Conclusion

The paper presents an approach based on the diffusion-segregation equation, which allows modeling the evolution of Zn dopant concentration profile in InGaAs/InAlAs/InP heterostructures. To conduct the research, a series of InGaAs/InAlAs/InP heterostructures with various designs were fabricated using different process parameters for vapor phase Zn diffusion from a DEZn metal-organic source. The diffusion-segregation parameters of materials and layers of heterostructures were determined from experimental distributions of electrically active dopants using ECV method. The proposed model allows one to qualitatively and quantitatively calculate Zn concentration profiles in InGaAs–InAlAs–InGaAs–InP heterostructures under various process parameters of Zn vapor phase diffusion. The diffusion coefficients in InGaAs/InAlAs/InP structures found from the analysis, and the dependence of the segregation coefficient distribution on the depth of the dopant occurrence demonstrated their dependence not only on temperature, but also on pressure. The values

of the established diffusion coefficients for diffusion from the vapor phase using DEZn are comparable with similar values for other diffusion methods presented in the scientific literature. It was found that at low temperatures and pressures, the thickness of InAlAs etch-stop layer had a significant effect on the depth of dopant occurrence, but it declined with increasing temperature and/or pressure due to the rise in diffusion coefficients in InP and InGaAs materials. The analysis of experimental results within the proposed diffusion model demonstrated the need to account for the contribution of segregation in the diffusion processes of Zn in InGaAs/InAlAs/InP heterostructures.

Funding

The authors thank Russian Railways for the financial support in fabrication of InGaAs/InAlAs/InP heterostructure samples for comprehensive studies of Zn vapor phase diffusion process. The computational modeling of the diffusion processes supported by the Ministry of Science and Higher Education of the Russian Federation (project reference number FSER-2025-0005).

Conflict of interest

The authors declare that they have no conflict of interest.

References

[1] V.V. Andryushkin, A.G. Gladyshev, A.V. Babichev, E.S. Kolodeznyi, I.I. Novikov, L.Ya. Karachinsky, N.A. Maleev, V.P. Khvostikov, B.Ya. Ber, A.G. Kuzmenkov. J. Phys.: Conf. Ser., **2103**, 012184 (2021). DOI: 10.1088/1742-6596/2103/1/012184

[2] A. Ozcan-Atar, A. Gocalinska, P.P. Michałowski, M. Johnson, J. O'Hara, B. Corbett, A. Rejmer, F. Peters, D.D. Vvedensky, A. Zangwill, G. Juska, E. Pelucchi. Appl. Surf. Sci., **688**, 162360 (2025). DOI: 10.1016/j.apsusc.2025.162360

[3] M.O. Petrushkov, M.S. Aksenov, D.B. Bogomolov, E.A. Emelyanov, D.Yu. Protasov, M.A. Putyato, I.B. Chistokhin, V.V. Preobrazhensky, A.M. Gilinsky, K.O. Voropaev. Optichesky zhurnal. **91** (2), 40 (2024) (in Russian). DOI: 10.17586/1023-5086-2024-91-02-40-49 [M.O. Petrushkov, M.S. Aksenov, D.B. Bogomolov, E.A. Emelyanov, D.Y. Protasov, M.A. Putyato, I.B. Chistokhin, V.V. Preobrazhenskii, A.M. Gilinsky, K.O. Voropaev. J. Opt. Technol., **91** (2), 86 (2024). DOI: 10.1364/JOT.91.000086].

[4] K. Lee, K. Yang. IEEE Phot. Techn. Lett., **26** (10), 999 (2014). DOI: 10.1109/LPT.2014.2312022

[5] Y. Chen, Z. Zhang, G. Miao, H. Jiang, H. Song. Phys. Status Solidi A, **219** (2), 2100577 (2022). DOI: 10.1002/pssa.202100577

[6] V.V. Preobrazhensky, I.B. Chistokhin, M.A. Putyato, N.A. Valisheva, E.A. Emelyanov, M.O. Petrushkov, A.S. Pleshkov, I.G. Neizvestniy, I.I. Ryabtsev. Avtometriya, **57** (5), 48 (2021) (in Russian). DOI: 10.15372/AUT20210506 [V.V. Preobrazhenskii, I.B. Chistokhin, M.A. Putyato, N.A. Valisheva, E.A. Emelyanov, M.O. Petrushkov, A.S. Pleshkov, I.G. Neizvestny, I.I. Ryabtsev. Optoelectron. Instrum. Data Process., **57** (5), 485 (2021). DOI: 10.3103/S8756699021050125].

[7] D.-H. Jun, H.-Y. Jeong, Y. Kim, C.-S. Shin, K.H. Park, W.-K. Park, M.-S. Kim, S. Kim, S.W. Han, S. Moon. J. Korean Phys. Soc., **69** (8), 1341 (2016). DOI: 10.3938/jkps.69.1341

[8] O.J. Pitts, M. Hisko, W. Benyon, S. Raymond, A.J. Springthorpe. J. Cryst. Growth, **393**, 85 (2014). DOI: 10.1016/j.jcrysgro.2013.09.0.53

[9] D.D. Agostino, G. Carnicella, C. Ciminelli, P. Thijs, P.J. Veldhoven, H. Ambrosius, M. Smit. Opt. Express, **23** (19), 25143 (2015). DOI: 10.1364/OE.23.025143

[10] M.O. Petrushkov, M.A. Putyato, I.B. Chistokhin, B.R. Semyagin, E.A. Emel'yanov, M.Yu. Esin, T.A. Gavrilova, A.V. Vasev, V.V. Preobrazhenskii. Techn. Phys. Lett., **44** (7), 612 (2018). DOI: 10.1134/S1063785018070258

[11] S.A. Blokhin, R.V. Levin, V.S. Epoletov, A.G. Kuzmenkov, A.A. Blokhin, M.A. Bobrov, Y.N. Kovach, N.A. Maleev, E.V. Nikitina, V.V. Andryushkin, A.P. Vasil'ev, K.O. Voropaev, V.M. Ustinov. Mater. Phys. Mech., **51** (4), 66 (2023). DOI: 10.18149/MPM.5142023_6

[12] K. Vanhollebeke, M. D'Hondt, I. Moerman, P. Van Daele, P. Demeester. J. Electron. Mater., **30**, 951 (2001). DOI: 10.1007/BF02657716

[13] D. Franke, F.W. Reier, N. Grote. J. Cryst. Growth, **195** (1–4), 112 (1998). DOI: 10.1016/S0022-0248(98)00681-2

[14] O.J. Pitts, W. Benyon, D. Goodlich, A.J. Springthorpe. J. Cryst. Growth, **352** (1), 249 (2012). DOI: 10.1016/j.jcrysgro.2011.10.006

[15] C.A. Hampel, C. Blaauw, J.E. Haysom, R. Glew, I.D. Calder, S. Guillon, T. Bryskiewicz, N. Puetz. J. Vac. Sci. Techn. A, **22** (3), 916 (2004). DOI: 10.1116/1.1640392

[16] P.L. Gareso. Indonesian. J. Phys., **20** (2), 21 (2009). DOI: 10.5614/itb.ijp.2009.20.2.1

[17] A. van Geelen, T.M.F. De Smet, T. van Dongen, W.M.E.M. van Gils. J. Cryst. Growth, **195** (1–4), 79 (1998). DOI: 10.1016/S0022-0248(98)00628-9

[18] J. Wisser, M. Glade, H.J. Schmidt, K. Heime. J. Appl. Phys., **71** (7), 3234 (1992). DOI: 10.1063/1.350969

[19] L. Zhang, X. La, X. Zhu, J. Guo, L. Zhao, W. Wang, S. Liang. IEEE J. Select. Top. Quant. Electron., **28** (2), 1 (2022). DOI: 10.1109/JSTQE.2021.3072702

[20] G. Tsamo Tagougue, M. Veillerot, E. Martinez, V. Thoréton, M. Martin, T. Baron, G. Lefevre, S. Cavalaglio, F. Bassani. J. Vac. Sci. Techn. B, **43** (3), 033204 (2025). DOI: 10.1116/6.0004489

[21] P.E. Kopytov, I.A. Starkov, I.I. Novikov, S.A. Blokhin, D.S. Papylev, R.V. Levin, V.V. Andryushkin, Ya.N. Kovach, E.V. Nikitina, K.O. Voropaev, L.Ya. Karachinsky. Pis'ma ZhTF, **50** (22), 48 (2024) (in Russian). DOI: 10.61011/PJTF.2024.22.59136.20059 [P.E. Kopytov, I.A. Starkov, I.I. Novikov, S.A. Blokhin, D.S. Papylev, R.V. Levin, V.V. Andryushkin, Ya.N. Kovach, E.V. Nikitina, K.O. Voropaev, L.Ya. Karachinsky. Techn. Phys. Lett., **50** (11), 99 (2024). DOI: TPL.2024.11.59678.20059].

[22] O.V. Alexandrov, A.A. Krivoruchko. Kondensirovannye sredy i mezhfaznye granitsy, **7** (2), 109 (2005) (in Russian). http://www.kcmf.vsu.ru/resources/t_07_2_2005_001.pdf

[23] F. Didley, M.C. Amann, R. Treichler. Jpn. J. Appl. Phys., **29** (5), 810 (1990). DOI: 10.1143/JJAP.29.810

[24] H.M. You, U.M. Gosele, T.Y. Tan. J. Appl. Phys., **74** (4) 2461 (1994). DOI: 10.1063/1.354683

[25] R. Gafiteanu, H.-M. You, U. Göesele, T.Y. Tan. MRS Online Proc. Library, **318**, 31 (1993). DOI: 10.1557/PROC-318-31

[26] B. Tuck. J. Phys. D: Appl. Phys., **18** (4), 557 (1985). DOI: 10.1088/0022-3727/18/4/002

[27] S.A. Blokhin, R.V. Levin, V.S. Epoletov, A.G. Kuzmenkov, A.A. Blokhin, M.A. Bobrov, Y.N. Kovach, N.A. Maleev, N.D. Prasolov, M.M. Kulagina, A.Yu. Guseva, Yu.M. Zadiranov, E.V. Nikitina, V.V. Andryushkin, A.P. Vasil'ev, K.O. Voropaev, V.M. Ustinov. Mater. Phys. Mech., **51** (5), 142 (2023). DOI: 10.18149/MPM.5152023_14
[28] P.E. Kopytov, S.A. Blokhin, D.S. Papylev, R.V. Levin, V.V. Andryushkin, Ya.N. Kovach, N.A. Maleev, A.I. Baranov, E.V. Nikitina, A.Yu. Andreev, I.V. Yarotskaya, A.A. Marmalyuk, M.A. Ladugin, K.O. Voropaev, A.F. Tsatsul.nikov, I.I. Novikov, L.Ya. Karachinsky. Bull. Lebedev Phys. Inst. **52** (Suppl 9), S974 (2025). DOI: 10.3103/S1068335625603905
[29] K. Lee, K. Yang, Phys. Status Solidi C, **10** (11), 1445 (2013). DOI: 10.1002/pssc.201300178
[30] A.I. Kurnosov, V.V. Yudin. *Tekhnologiya proizvodstva poluprovodnikovyh priborov i integral'nyh skhem* (M. Vyssh. shkola, M., 1979) (in Russian).
[31] A. Azarov, V. Venkatachalapathy, L. Vines, E. Monakhov, In-H. Lee, A. Kuznetsov. Appl. Phys. Lett., **119** (18), 182103 (2021). DOI: 10.1063/5.0070045
[32] B.S. Bokshteyn. *Diffuziya v metallakh* (M. Metallurgiya, 1978) (in Russian).
[33] G.J. van Gurp, P.R. Boudewijn, M.N.C. Kempeners, D.L.A. Tjaden. J. Appl. Phys., **61**, 1846 (1987). DOI: 10.1063/1.338028
[34] H. Ando, N. Susa, H. Kanbe. IEEE Trans. Electron Dev., **29** (9), 1408 (1982). DOI: 10.1109/T-ED.1982.20890
[35] M.H. Ettenberg, M.J. Lange, A.R. Sugg, M.J. Cohen, G.H. Olsen. J. Electron. Matter., **28**, 1433 (1999). DOI: 10.1007/s11664-999-0136-5
[36] U. Schade, P. Enders. Semicond. Sci. Technol., **7**, 752 (1992). DOI: 10.1088/0268-1242/7/6/006
[37] F. Schmitt, L.M. Su, D. Franke, R. Kaumanns. IEEE Trans. Electron Dev., **31** (8), 1083 (1984). DOI: 10.1109/T-ED.1984.21665
[38] N. Arnold, R. Schmitt, K. Heime. J. Phys. D: Appl. Phys., **17**, 443 (1983). DOI: 10.1088/0022-3727/17/3/006
[39] M. Wada, M. Seko, K. Sakakibara, Y. Sekiguchi. Jpn, J. Appl. Phys., **28** (10), L1700 (1989). DOI: 10.1143/JJAP.28.L1700
[40] M. Razeghi, M.A. Poisson, J.P. Larivain, J.P. Duchemin. J. Electron. Mater., **12** (6), 371 (1983). DOI: 10.1007/BF02651138

Translated by T.Zorina